Comparison of Bone Quality in Middle Ages and Late Modern Period Human Skeletons from Latvia

Ksenija Šerstņova [1], Edgars Edelmers [1,*], Maksims Zolovs [2,3] and Māra Pilmane [1,*]

[1] The Institute of Anatomy and Anthropology, Rīga Stradiņš University, LV-1010 Riga, Latvia; ksenija.serstnova@rsu.lv
[2] Statistics Unit, Rīga Stradiņš University, LV-1007 Riga, Latvia; maksims.zolovs@rsu.lv
[3] Institute of Life Sciences and Technology, Daugavpils University, LV-5401 Daugavpils, Latvia
[*] Correspondence: edgars.edelmers@rsu.lv (E.E.); mara.pilmane@rsu.lv (M.P.)

Abstract: The analysis of bone microstructure and histological examination currently provides valuable insights into various facets of bone biology, ancient human existence, and bone-related diseases. This study aims to scrutinize the microstructure of historic Latvian bones, with three bone element groups selected (humerus, radius, and ulna) from a skeletal collection spanning from the Middle Ages to the Late Modern Period, procured through an archaeological excavation at St. George's Church in Riga. To evaluate the changes in bone samples over time, two methods are utilized: (i) micro-computed tomography, used for measuring and calculating bone volume/trabecular volume (BV/TV), cortical bone and trabecular thickness, and trabecular pore diameter; (ii) immunohistochemistry (IHC) is employed to detect the presence of Runx2, OPG, OC, MMP2, TIMP2, BFGF, IL-1, IL-10, OPN, defensin-2, BMP 2/4, TGFβ factor in bone cells—specifically osteocytes. Archaeological human bone remains from the Middle Ages period in Latvia display a decline in the average bone volume to trabecular volume ratio when compared with the Late Modern Period, indicating a potential reduction in bone quality in the skeletons, potentially associated with a lower living standard during the earlier era. Comparing factors between the periods reveals a higher value of TIMP2 ($p = 0.047$) in samples from the Late Modern Period group, while IL-1 is higher ($p = 0.036$) in the Middle Ages group, which may suggest the presence of disease and diminished bone quality in the skeletons from the Middle Ages.

Keywords: bone microstructure; micro-computed tomography; immunohistochemistry; tissue factors

1. Introduction

The analysis of ancient bone remains initiates with a macroscopic evaluation, which is subsequently followed by the identification of their histomorphological structure and comprehension of the bone formation and resorption processes. Bone, categorized as a type of connective tissue, comprises various cell types and an expansive extracellular matrix encompassing the bone cells [1]. Osteocytes are cells that are necessary for maintaining bone homeostasis in the human skeleton, are the most numerous (90–95%), and develop through the osteoblast differentiation process, which occurs together with cell morphological and ultrastructural changes [2,3]. Mature osteocytes are located in lacunae and are interconnected with adjacent osteocytes and other bone cells by their dendritic processes extended in canaliculi, as a result forming a canalicular system (LCS) for cell communication. This system provides osteocytes with oxygen and nutrients, coming from closely located blood vessels, as well as enables intercellular transport of small signaling molecules between the bone cells [4,5].

1.1. Bone Tissue Factors and Proteins

As active and multifunctional bone cells, osteocytes are involved in numerous physiological processes induced by different factor/protein expressions in and outside bone

tissue. First, osteocytes take part in several processes related to bone formation and participate in the synthesis and mineralization of osteoid matrix by producing proteins such as osteocalcin (OCN) and alkaline phosphatase (ALP). In places of bone tissue damage, they are known to secrete osteopontin (OPN) for the induction of new bone formation. By releasing signaling molecules through LCS, osteocytes are capable of inhibiting or stimulating osteoblasts and, thus, of regulating bone formation. Secondly, osteocytes take part in osteoclastogenesis by secreting RANKL, which is essential for normal bone remodeling, and osteoprotegerin (OPG), which protects the skeleton from extensive osteoclastic bone resorption [2,6]. Thirdly, bone tissue is an important reservoir of calcium, and under the induction of parathyroid hormone (PTH), osteocytes cause local demineralization and the further release of calcium in the bloodstream. Together with other functions, the osteocyte is considered to be a mechanosensory and mechanotransducer cell, as it is capable of responding to mechanical stimuli and loads. Moreover, osteocytes tend to act as endocrine cells that secrete sclerostin protein, which promotes bone resorption, and fibroblast growth factor-23 (FGF-23), the phosphate regulator, in response to increased levels of phosphate in serum [5,7].

Among all previously mentioned factors and proteins that give osteocytes the ability to regulate the activity of osteoblast, osteoclasts, as well as bone remodulation processes, and some other factors can be detected in osteocytes. The process of osteoblasts differentiation into osteocytes is under the control of several transcription factors, such as runt-related transcription factor 2 (Runx2), which can further be expressed by osteocytes [8]. Transforming growth factor β (TGF-β) is predominantly found in osteoblasts but is also detected in osteocytes of human and animal bone tissue. Moreover, TGF-β2 and TGF-β3 isoforms play a role in endochondral and intramembranous bone formation, as they signal to promote osteoprogenitor cell proliferation as well as differentiation into the osteoblasts [9,10]. Heino et al., 2002 [11], found that TGF-β secreted by mouse osteocytes inhibits osteoclastogenesis and osteoclastic bone resorption without affecting the number of mature osteoclasts. Bosetti et al., 2007 [12], proved that cooperation between TGF-β and basic fibroblast growth factor (FGF/FGF-2) also induces osteoblast proliferation as well as inhibits ALP activity with osteoblast mineralization. Expressed by periosteal cells, osteoblasts, and osteocytes, and stored in ECM, FGF-2 is important for bone development, maintenance, and fracture healing, as disruption of the FGF-2 gene in mice causes a decrease in bone formation [13,14]. Bone morphogenetic proteins (e.g., BMP2, BMP4) are members of the TGF-β superfamily that among many functions also play an important role in bone formation. Runx2 is essential for BMP-2 to promote osteoblast differentiation and maturation [9,10]. As for matrix metalloproteinase-2 (MMP-2) and tissue inhibitors of metalloproteinases-2 (TIMP-2), they need to cooperate in a balanced manner for normal bone development. MMP-2 is an enzyme responsible for ECM degrading, while TIMP-2 can inhibit the catalytic activity of MMP-2 at its high concentrations and activate pro-MMP-2 at low concentrations, as dysregulation of MMP-2/TIMP-2 expression may lead to pathological conditions [15].

Under bone infection and inflammatory conditions, both innate and adaptive immune cells can regulate bone resorption by secreting different inflammatory (IL-1β, TNF-α, IL-6, IL-17) and anti-inflammatory factors (IL-4, IL-10, and gamma interferon). Inflammatory cytokines stimulate osteoclast formation through the induction of RANKL, while anti-inflammatory cytokines inhibit osteoclastogenesis and prevent bone loss [16].

Although the impact of those numerous factors/proteins/cytokines on bone cells and ECM properties provide us with relevant information about the process of bone formation and resorption during embryogenesis, in post-natal life, and within the chronological-related changes, there is a lack of data on their presence in samples of archeological human remains. One of the topics of fossil bone studies is related to the analysis of proteins (collagen, osteocalcin), as they can survive for a long period of time and provide us with information about the ancient human paleo diet and bioarchaeology. Schmidt-Schultz and Schultz [17,18], in a series of research on human archaeological bone, separated ECM proteins (collagen, osteonectin, osteopontin, and alkaline phosphatase) via electrophoresis

and noticed that their quality is the same as that of recent bones. Schmidt-Schultz and Schultz [19] extracted growth factors (insulin growth factor II (IGF-II), BMP-2, and TGF-b) from ancient compact human bone and tooth dentin and suggested that macroscopic and microscopic analysis in combination with biochemical techniques could allow us to obtain more information about the history and evolution of diseases. Smith et al. [20] in their study used ELISA to determine the relative amount of OCN in the animal bone and noticed that its amount decreases with the increase in diagenetic bone changes. Scott et al. [21] analyzed human femur cortical bone samples using ELISA and did not find any correlation between osteocalcin concentrations and diagenesis, suggesting that the protein can survive across a range of time periods and variable burial environments. It is noticeable that preservation conditions, such as age, humidity, temperature, pH, microorganism invasion, and burial context, may also affect the quality of bone tissue [22].

1.2. Bone Microstructure

As for the bone microstructure of ancient human bone samples, it is widely studied by osteoarcheologists and biological anthropologist investigators to answer questions about people from the past, their habitat, socioeconomic status, life quality, and diseases in comparison with modern conditions [23,24]. The most common techniques for such studies are computed tomography and/or X-ray radiography, as well as the usage of high-powered microscopes to examine the remains. All these techniques allow us to obtain detailed information and visual pictures of bones, without affecting or breaking them [25].

The understanding and studies of bone microstructural change, e.g., osteon population density (OPD), osteon area (On.Ar), bone volume (BV/TV), trabecular number (Tb.N), trabecular thickness (Tb.Th), and trabecular spacing/pore size (Tb.Sp), provides us with interesting data about the health status of populations and pathological and living conditions of the past [26]. Ancient human skeletons from archaeological sites are a rich source of information on the history of numerous bone diseases, e.g., skeletal dysplasia [27], Paget's disease [28,29], and osteoporosis. Osteoporosis is one of the most widely examined pathologies of skeletal system change in the study of both the past and the present [30,31].

Not only diet but also lifestyle activities can affect the skeletal system, as exercise is known to increase bone density and improve overall bone health. Chirchir et al. [32] results showed that among chimpanzees, Australopithecus africanus, Paranthropus robustus/early Homo, Homo neanderthalensis, and early Homo sapiens, only recent modern humans have low trabecular density throughout the limb joints, potentially resulting from increased sedentism and reliance on technological and cultural innovations. Later, Chirchir and his colleagues [33] subsequently found that the decrease in physical activities, which came about due to the shift towards farming and industrial practices, played a significant role in the diminished bone density observed in contemporary humans compared to their Holocene predecessors. Gosman and Ketcham [34] conducted a research study on skeletal samples of subadult and young adult individuals from the Late Prehistoric Ohio Valley. Their investigation revealed distinct and interconnected patterns of growth, development, general functional activities, trabecular distribution, and the architecture of the bones. Pitfield et al. [35] also noticed differences in skeletal samples of children from medieval England, as after 7 years of age low-status children from York or Newcastle had more habitual loading on their arm bones than the high-status children in Canterbury, resulting from physical activities as the former entered the workforce.

The combination of Micro-CT imaging technique and histological analysis offers a powerful approach to scientific investigations, particularly when using the Zeiss Xradia Versa 3D X-ray microscopes (XRM)—it is highly versatile and capable of producing superior 3D image quality for a broad array of materials under different conditions. Importantly, this allows for the preservation and continued use of valuable samples, enabling studies that require four-dimensional visualization and in situ analysis. When Micro-CT imaging is combined with histological analysis, it allows for a complementary study of both the macroscopic and microscopic structures of the sample. Histological analysis can provide

detailed insights into the cellular level structure and organization, while Micro-CT gives an overview of the overall structural organization in three dimensions. This combination can provide a more holistic and in-depth understanding of the sample, offering superior insights that might not be obtainable when using each technique in isolation [36].

1.3. Socioeconomic History of Riga in the 14–15th and 18–19th Centuries

Riga was an important trade center in the 14th and 15th centuries and experienced both social and economic changes during this time. Socially, Riga was a multi-ethnic city, with Latvians and Germans, living alongside each other, but the data on its demography in the Middle Ages is scarce. It is estimated that the number of its citizens at the time varied from around 6000 to 8000, and their lifespan and welfare were affected by local wars and plague epidemics [37]. Nevertheless, the city was rapidly developing and changing according to the safety and well-being needs of the population. A major role in Riga's economic development was played by the city's geographical location, as proximity to the harbor encouraged transit trade. Riga was a major center for the trade of goods, such as timber, furs, and amber. The city was part of the Hanseatic League, a powerful economic alliance of trading cities in Northern Europe. However, the 14th and 15th centuries were also marked by various social and economic crises. In the mid-14th century, a plague epidemic devastated Riga's population and led to a decline in economic activity. The city also faced political instability, with conflicts between the city's ruling class and the Archbishop of Riga. According to traditions and city laws, society was divided into four orders: clergy, merchants, artisans, and servants [38,39].

In the Middle Ages, the city's population was negatively affected by the Northern War and plague. In the first half of the 18th century the number of civilians in Riga increased by more than 40,000. However, Riga was an important commercial and cultural center in the 18th and 19th centuries with a rapidly developing city infrastructure and intensive growth of its manufacturing sector. The abolition of many restrictions and rapid development of medicine and industry, such as metalworking, mechanical engineering, chemical industry, and production of fabric, paper, porcelain, and cork, stimulated the urbanization of the area, and at the end of the 19th century, Riga had almost 300,000 citizens. Riga's economic growth was also supported by rising education and culture (building schools and universities) [40].

The study aimed to investigate the microstructure of Latvian historic bone specimens by using Micro-CT and IHC methods and to evaluate possible differences in analyzed factor expression and bone structure between Late Modern Period and Middle Ages groups.

2. Materials and Methods

2.1. Bone Samples

The bones used in this study were carefully selected from a skeletal collection that was obtained by archeological excavation in 1983–1985 from the St. George's Church in Riga, Latvia. For further examination within the study, three bone elements were chosen: humerus, radius, and ulna. All samples lack visible effects of diagenesis and belong to different time periods dating from the Middle Ages till the Late Modern Period. For the Late Modern Period group (1750–1945 CE), five ulnae (two males that were approximately 40–55 years old, one male about 55+ years old, as well as one female that was around 15–18 years old, along with another female one approximately 55+ years old) and four radii were selected (two males and females that were approximately 20–25 years old). For the Middle Ages group (1300–1400 CE), 14 ulnae, 10 humeri, and 9 radii were chosen (14 females and 19 males), 11 of them from individuals aged 15–25 years (not finished ossification) and 22 individuals aged of 30–55+ (after the skeleton ossification). Overall, 8 out of 33 showed skeleton changes, with dominating vertebral changes. No age/sex differences were visualized and, thus, included in the common evaluation [41].

2.2. Micro-Computed Tomography

All the subjects' bones were measured with Micro-CT 3D imaging technique to evaluate chronological-related changes in bone microstructure using Zeiss Xradia 510 Versa system. Micro-CT observations of bone samples were conducted at the Daugavpils University, Daugavpils, Latvia. All Micro-CT scans were executed employing a polychromatic X-ray beam with an energy rate of 80 kV and power of 7 W. Images were imported into Dragonfly PRO (ver. 2020.1) software platform for interactive segmentation and 3D visualization.

The Otsu function was used to segment different densities of bone and air regions in the image for the measurement of the bone volume to trabecular volume ratio (BV/TV) (Figure 1) [42]. The BV/TV ratio was calculated for five squares of equal volume (0.5 cm^3), and the obtained results were used to calculate the average value. Using the same thresholding method, a mask was made that was overlaid with the original image, and 15 measurements of trabecular thickness perpendicular to the trabecula and 15 measurements of trabecular pore diameters were made. All measurements were randomly taken across various planes in the epiphysis of the bones. Cortical bone thickness measurements were carried out identically to trabecular thickness, but instead of 15 measurements, 5 were taken in one plane that was strictly perpendicular to the bone shaft.
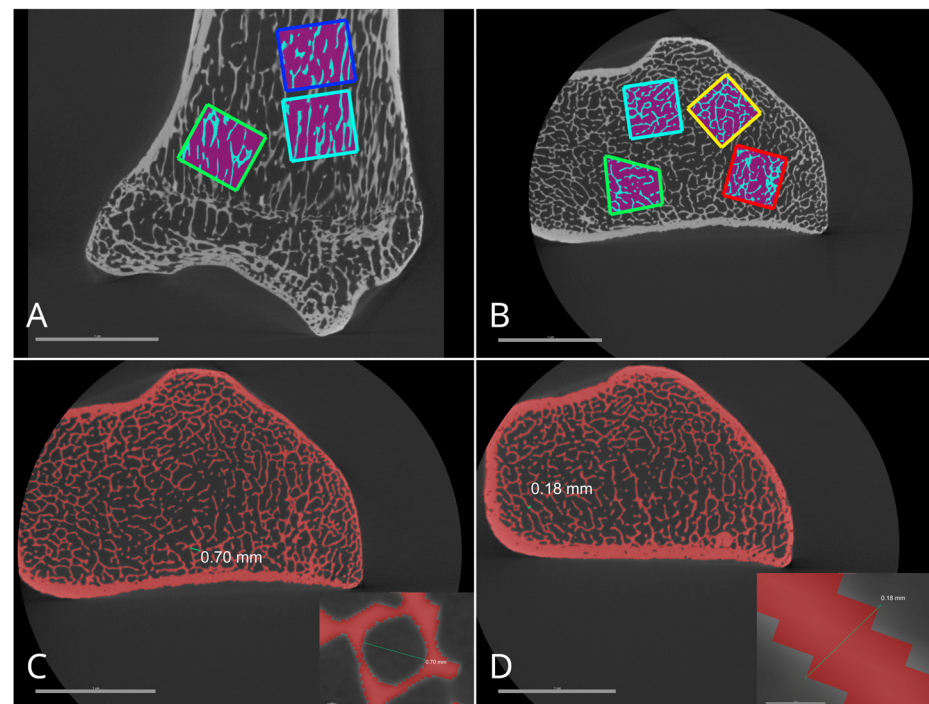
Figure 1. Measurements for bone volume/trabecular volume ratio calculations in ulna using Otsu method (**A**,**B**). Subfigures depict the trabecular pore diameter (**C**) and trabecular thickness (**D**).

2.3. Immunohistochemistry

Research samples were obtained from the metaphysis of all bones. Bone fragments were decalcified using Biodec R (UN3264, Bio-optics) and fixed in 10% buffered formaldehyde. After that, they were dehydrated in different concentrations of alcohol and embedded in paraffin. As the last manipulation, the paraffin block was cut into 3–5 μm thick sections using the Leica RM2245 Microtome [43].

The IHC method was performed to detect the presence of the following factors in the bone cells (osteocytes): Runx2 (ab192566, 1:100, Abcam, Cambridge, UK), OPG (orb120312, 1:100, Biorbyt LLC, San Francisco, CA, USA), OC (orb259644, 1:100, Biorbyt LLC, San Francisco, CA, USA), MMP2 (orb101049, 1:100, Biorbyt LLC, San Francisco, CA, USA), TIMP2 (sc-21735, 1:50, Santa Cruz, Santa Cruz, CA, USA), BFGF (ab16828, 1:200, Abcam, Cambridge, UK), IL-1a (orb33640, 1:100, Biorbyt LLC, San Francisco, CA, USA), IL-10 (orb100193,

1:600, Biorbyt LLC, San Francisco, CA, USA), OPN (orb11191, 1:100, Biorbyt LLC, San Francisco, CA, USA), β-defensin-2 (sc-20798, 1:100, Santa Cruz, Santa Cruz, CA, USA), BMP 2/4 (AF355, 1:100, R&D Systems, Wiesbaden, Germany), TGFβ (orb77216, 1:100, Biorbyt LLC, San Francisco, CA, USA) [36]. Microslides with bone tissue samples were evaluated using the Leica DC 300F camera and image processing and analysis software Image-Pro Plus v.6.0 (Media Cybernetics, Rockville, MD, USA). The calculation of positively stained cells for each investigated IHC marker was performed via a semi-quantitative scoring method [44]. Amount of positively stained cells in tissue samples were graded by the following scale: 0—no positive structures; 0/+—occasional positive structures; +—a few positive structures; +/++—few to moderate number of positive structures; ++—moderate number of positive structures; ++/+++—moderate to numerous positive structures; +++—numerous positive structures; +++/++++—numerous to abundant structures; ++++—an abundance of positive structures [45].

2.4. Statistics

All results from semi-quantitative evaluated scoring were transformed into numerical form as follows: 0: equals 0, 0/+: equals 0.5, +: equals 1, +/++: equals 1.5, ++: equals 2, ++/+++: equals 2.5, +++: equals 3, +++/++++: equals to 3.5, ++++: equals to 4. The Mann–Whitney U test was used to compare IHC value differences between two independent groups (Late Modern Period and Middle Ages), and Spearman's rank correlation coefficient was calculated to detect correlations between the factors and/or Micro-CT parameters in the Middle Ages group, with the following interpretation: r = 0–0.19—very weak correlation, r = 0.2–0.39—weak correlation, r = 0.4–0.59—moderate correlation, r = 0.6–0.8—strong correlation and r = 0.8–1.0—a very strong correlation. While *t*-tests along with two-way ANOVA were used to compare the Micro-CT measurement data. SPSS version 22.0 (IBM Corp., Armonk, NY, USA) was used for statistical data analysis. *p* value < 0.05 was considered statistically significant.

3. Results

3.1. Exemplar Micrographs

Bone tissue samples from different time period groups reveal some destruction at peripheral sites of bone sections, which was more visible in the Middle Ages group (Figure 2A,B). Both Haversian and Volkmann's channels have irregularities and vary in size and diameters. The arrangement of lamellas in bone tissue is also variable (Figure 3A,B).
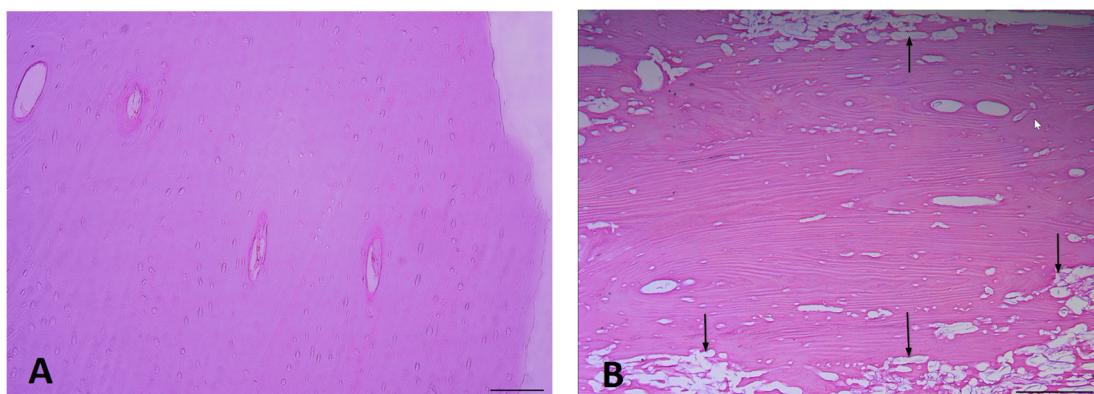
Figure 2. The appearance of bone tissue sample: (**A**) Late Modern Period bone destruction is rare (right humerus), (**B**) Middle Ages bone destruction (shown with arrows, left humerus) (H&E, ×100 magnification).
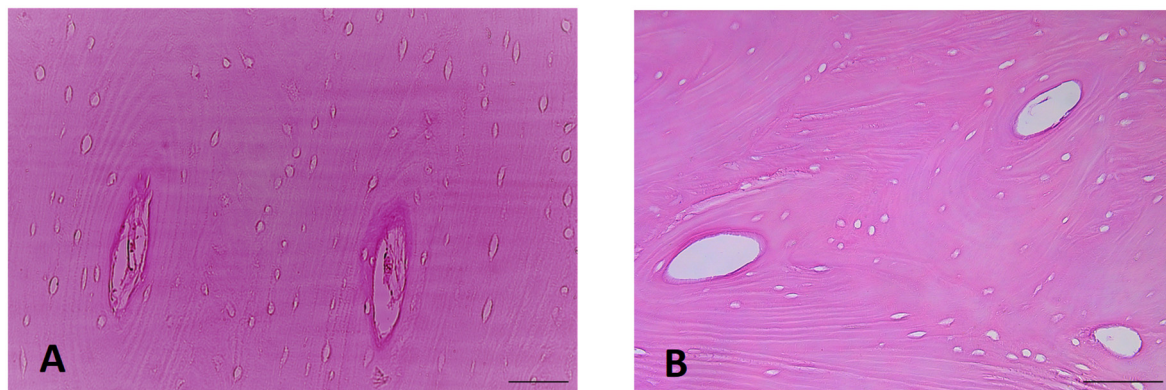
Figure 3. The appearance of practically unchanged bone tissue samples: (**A**) Late Modern Period bone lamellas (right humerus), and (**B**) Middle Ages bone lamellas (left humerus) (H&E, ×200 magnification).

3.2. IHC-Positive Cell Presence in Bone Tissue

Cells that are positive for all cytokines and factors can be seen in the majority of bone material samples (Table 1). Occasionally, OCN protein-positive cells are detected in the Middle Ages group (Figure 4A), while only a few such cells are detected in the Late Modern Period group (Figure 5A), with no significant difference between them. Both groups present an equal number (few) of OPN (Figures 4B and 5B) and OPG (Figures 4C and 5C) positive cells. The cytokine IL-10 is found only in a few osteocytes in both the Middle Ages (Figure 4D) and the Late Modern Period (Figure 5D) microslides.

Table 1. The mean number of TGF-β, OPN, MMP2, TIMP2, OPG, OCN, bFGF, Runx2, IL-10, BMP2/4, and βDef.2 positive cells in the bone samples of Late Modern Period and Middle Ages groups.

		TGFB	OPN	MMP2	TIMP2	OPG	OCN	bFGF	Runx2	IL-1a	IL-10	BMP2/4	βDef.2
Control group		+	+	+	+/++	+	+	+	0	0/+	+	+	0/+
	Mean	1.25	1	1	1.5	1	1	1	0	0.25	1.25	1.25	0.5
	SD	0.35	0.71	0.71	0	0.71	0.71	0	0	0.35	0.35	0.35	0.71
Patient group		0/+	+	+	+	+	0/+	+	0	+	+	+	+
	Mean	0.56	0.94	1.06	0.94	1	0.69	0.81	0.06	0.88	0.75	0.75	0.75
	SD	0.18	0.32	0.32	0.32	0.38	0.26	0.26	0.18	0.23	0.27	0.27	0.38

Abbreviations: TGFβ—transforming growth factor β; OPN—osteopontin; MMP2—matrix metalloproteinase-2; TIMP2—tissue inhibitor of metalloproteinases-2; OPG—osteoprotegerin; OCN—osteocalcin; βFGF—β-fibroblast growth factor, Runx2—runt-related transcription factor 2; IL-1a—interleukin 1a; IL-10—interleukin 10; BMP 2/4—bone morphogenetic proteins 2/4; βDef.2—β-defensin-2. No positive (0), occasional (0/+), few (+), few to moderate (+/++).

IL-1a immunoreactive cells are found in significantly higher numbers in the Middle Ages group (Figure 4E) than in the Late Modern Period group (Figure 5E), where they appear very infrequently. As for the factors, βFGF, BMP 2/4, and MMP2 all display a similar presence of few positive osteocytes in both analyzed groups (Figure 4F–H and Figure 5F–H). However, MMP2 shows significant relevance above TGFβ, OCN, and BMP 2/4.

The amount of beta-defensin-2 slightly varies in the Late Modern Period group (Figure 5I), while only a few factor-positive osteocytes are detected in the Middle Ages group (Figure 4I). A few positive TGFβ cells are observed in Late Modern Period samples (Figure 5J) compared to an occasional number in the Middle Ages group (Figure 4J), but the difference between the groups is not statistically significant.

Of all the analyzed factors, only TIMP2 presents a significantly higher (U = 1.000, $p = 0.047$) number of immunoreactive osteocytes in samples from the Late Modern Period group (Figure 5K) compared to the Middle Ages (Figure 4K) (Table 2).
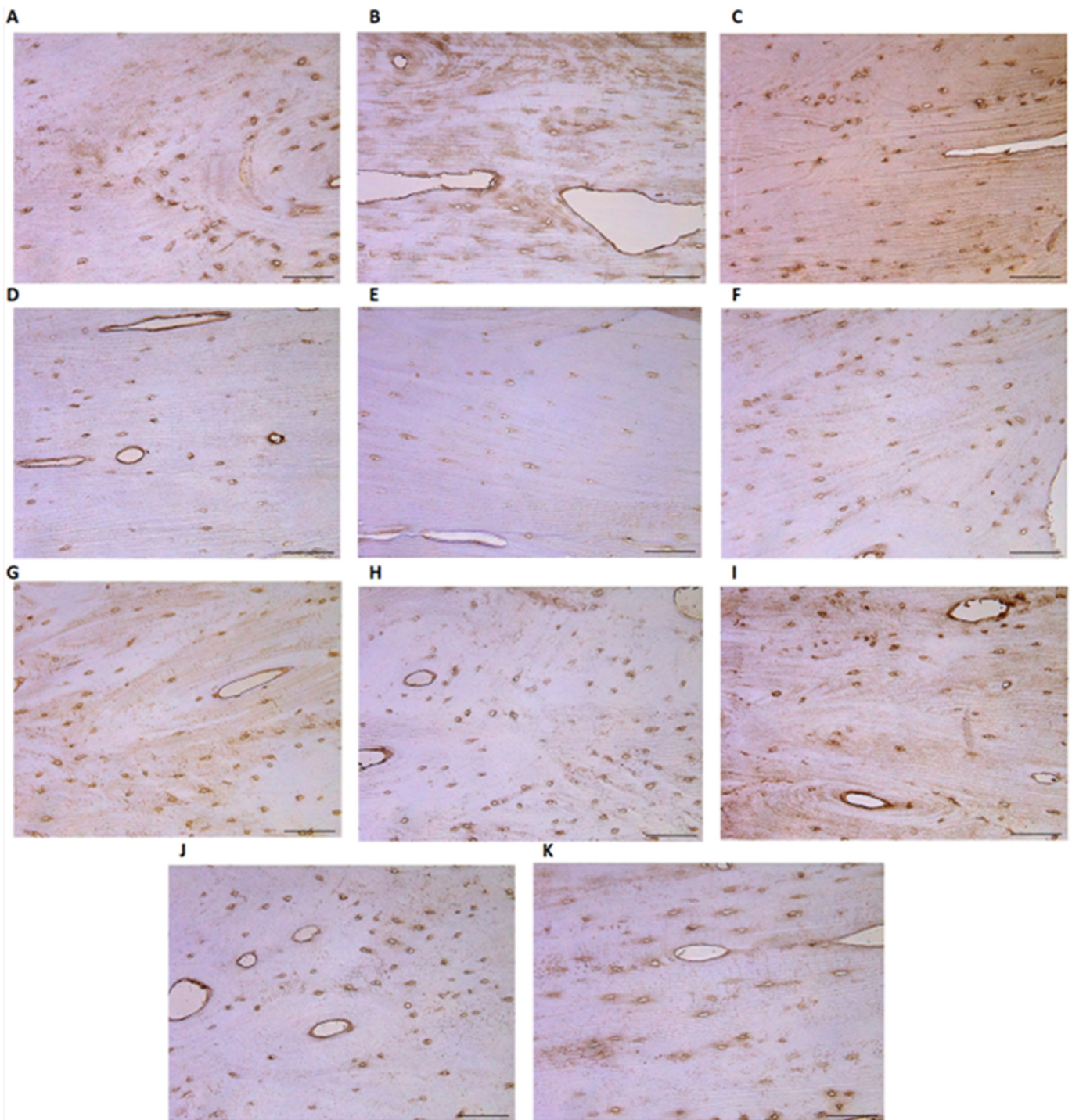
Figure 4. Evaluation of different tissue factors in the microslides (IHC ×200 magnification) of the Middle Ages bone tissue: (**A**) OCN (0/+), (**B**) OPN (+), (**C**) OPG (+), (**D**) IL-10 (+), (**E**) IL-1a (+), (**F**) βFGF (+), (**G**) BMP2/4 (+), (**H**) MMP2 (+), (**I**) βDef.2 (+), (**J**) TGFβ (0/+), and (**K**) TIMP2 (+). Abbreviations: No positive (0), occasional (0/+), few (+), few to moderate (+/++), moderate (++), moderate to numerous (++/+++), numerous (+++), numerous to abundant (+++/++++), and abundance (++++) of positive cells.
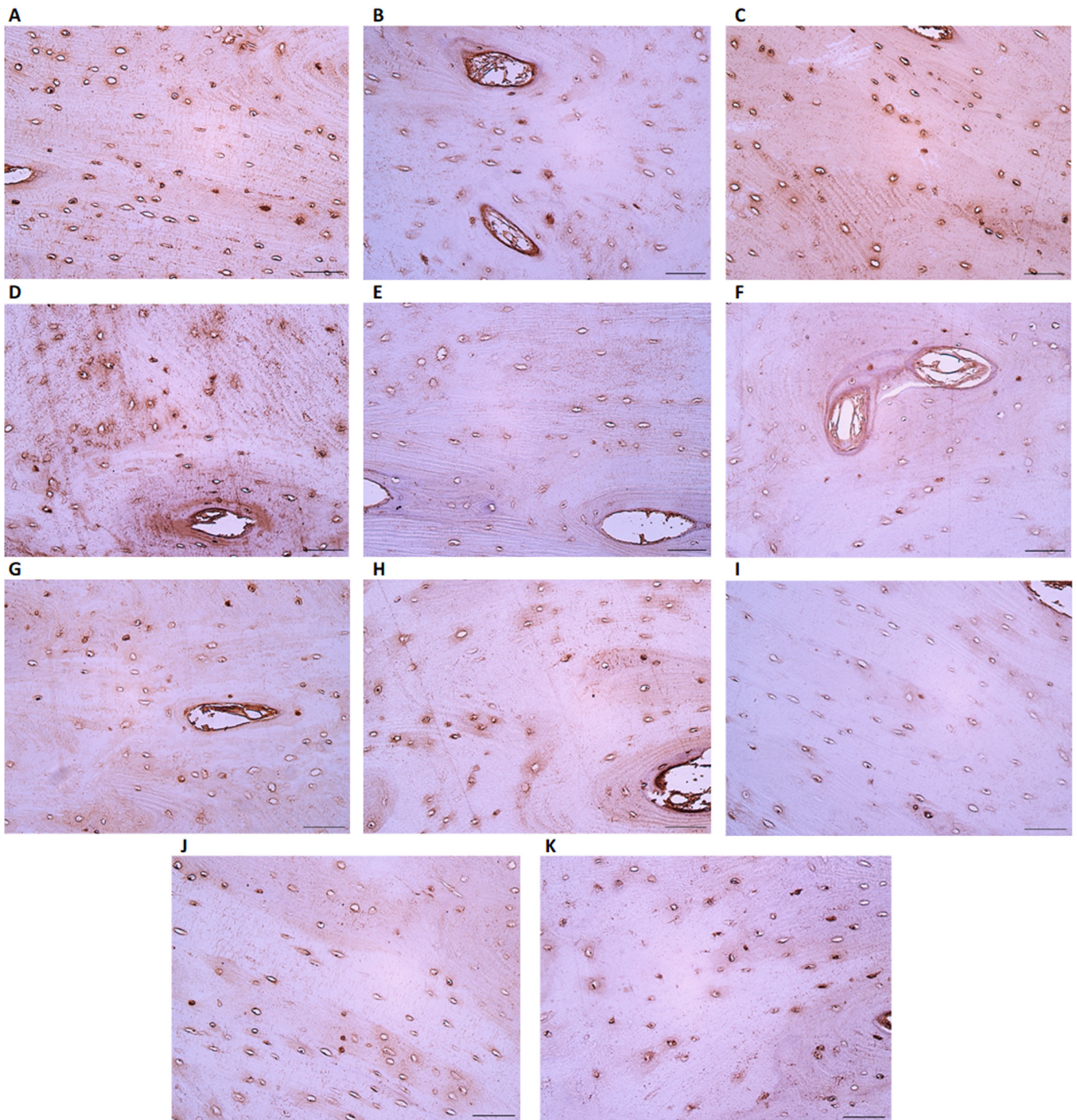
Figure 5. Evaluation of different tissue factors in the microslides (IHC ×200 magnification) of the Late Modern Period bone tissue: (**A**) OCN (+), (**B**) OPN (+), (**C**) OPG (+), (**D**) IL-10 (+), (**E**) IL-1a (0/+), (**F**) βFGF (+), (**G**) BMP2/4 (+), (**H**) MMP2 (+), (**I**) βDef.2 (0/+–+), (**J**) TGFβ (+), and (**K**) TIMP2 (+/++). Abbreviations: No positive (0), occasional (0/+), few (+), few to moderate (+/++), moderate (++), moderate to numerous (++/+++), numerous (+++), numerous to abundant (+++/++++), and abundance (++++) of positive cells.

Table 2. Mann–Whitney U test reveals statistically significant differences in factors between the Middle Ages and Late Modern Period bone samples.

Factor	Mann–Whitney U	Z-Score	*p*-Value
TIMP2	1	−1984	0.047
IL-1a	1	−2092	0.036

Abbreviations: TIMP2—tissue inhibitor of metalloproteinases-2; IL-1a—interleukin 1a.

Interestingly, almost no Runx2 positive cells are visible in the microscope field of both groups. Moreover, the statistical analysis indicates that all other cytokines/factors are more numerous (Z = −2414–−2640, *p* = 0.008–0.016) than Runx2 within Middle Ages bone samples, but no significant difference is found in the Late Modern Period group (Table 1).

3.3. Micro-CT Analysis

The mean bone volume to trabecular volume ratio is significantly higher in the 30–55+ years old group (30 ± 0.81) than in the 15–25 years old group (21.2 ± 2.47) for the Late Modern Period, with a statistically significant difference of 9.67, 95% CI [1.04–8.99], t (7) = 7.42, *p* ≤ 0.05, d = 4.99. Similarly, the mean thickness of trabecular bone is significantly higher in the 30–55+ years old group (191.5 ± 20.29) than in the 15–25 years old group (149.2 ± 19.05) for the Late Modern Period, with a statistically significant difference of 42.31, 95% CI [0.01–4.21], t (7) = 3.22, *p* ≤ 0.05, d = 2.16. However, the mean diameter of bone pores is significantly lower in the 30–55+ years old group (410.8 ± 25.64) than in the 15–25 years old group (528.9 ± 63.45) for the Late Modern Period, with a statistically significant difference of −118.10, 95% CI [−2.32 till −4.48], t (7) = −3.46, *p* ≤ 0.05, d = −2.32.

In the Middle Ages, the mean bone volume to trabecular volume ratio is significantly higher in the 30–55+ years old group (26.6 ± 3.87) than in the 15–25 years old group (23 ± 3.74), with a statistically significant difference of 3.61, 95% CI [0.16–1.71], t (31) = 2.55, *p* ≤ 0.05, d = 0.94.

Comparatively, the mean bone volume to trabecular volume ratio is significantly higher in the Late Modern Period (30.9 ± 0.81) than in the Middle Ages (26.6 ± 3.87) for the 30–55+ years old group, with a statistically significant difference of 4.30, 95% CI [0.22–8.37], t (24) = 2.18, *p* ≤ 0.05, d = 1.18.

There is a statistically significant interaction between the age groups (15–25 years old and 30–55+ years old) and the time period (Late Modern Period and Middle Ages) that impacts the mean bone volume to trabecular volume ratio, F (1, 38) = 4.95, *p* < 0.05, η2p = 0.12. This suggests that the impact of age group on the mean bone volume to trabecular volume ratio changes depending on the time period. Similarly, this interaction also affects the mean thickness of trabecular bone, F (1, 38) = 4.47, *p* < 0.05, η2p = 0.11, and the mean diameter of bone pores, F (1, 38) = 5.44, *p* < 0.05, η2p = 0.13. However, it is not possible to determine the values of the influence due to *p* for all the measurements being higher than 0.05.

For the Middle Ages, the mean diameter of bone pores is significantly lower in the male group (448.4 ± 58.91) than in the female group (495.8 ± 40.30), with a statistically significant difference of −47.37, 95% CI [−1.81 till −0.03], t (20) = −2.09, *p* ≤ 0.05, d = −0.91.

There is also a statistically significant interaction between the sexes (males and females) and the time period (Late Modern Period and Middle Ages) that affects the mean bone volume to trabecular volume ratio, F (1, 38) = 4.46, *p* < 0.05, η2p = 0.11. This indicates that the impact of sex on the mean bone volume to trabecular volume ratio changes depending on the time period. It is not possible to determine the values of the influence due to *p* for all the measurements being higher than 0.05.

The Micro-CT measurements are depicted in Table 3.

Table 3. Micro-CT measurements of Late Modern Period and Middle Ages bone samples made using Zeiss Xradia 510 Versa system.

Bone Name/Group	Sex	Age	Time Period	Mean Bone Volume to Trabecular Volume Ratio (%/0.5 cm^3)	Mean Thickness of Trabecular Bone (μm)	Mean Diameter of Bone Pores (μm)	Mean Thickness of Cortical Bone (μm)
Ulna	F	15–18	Late Modern Period	22.02	144.22	471.10	4690.98
Radius	M	20–25	Late Modern Period	20.35	150.63	614.98	3590.32
Radius	F	20–25	Late Modern Period	22.58	169.78	537.43	3585.83
Radius	M	20–25	Late Modern Period	23.76	161.50	558.43	3233.28
Radius	F	20–25	Late Modern Period	17.39	120.06	462.49	2903.22
Ulna	M	40–55	Late Modern Period	31.47	187.36	411.45	3518.14
Ulna	M	40–55	Late Modern Period	30.02	210.51	383.73	3555.34
Ulna	F	55+	Late Modern Period	30.39	164.81	445.10	3362.52
Ulna	M	55+	Late Modern Period	31.68	203.51	402.85	3564.94
Ulna	F	15–18	Middle Ages	23.46	175.46	375.77	3188.85
Humerus	F	15–18	Middle Ages	25.16	191.00	478.27	4575.80
Radius	F	15–18	Middle Ages	21.86	159.90	435.74	2930.25
Humerus	F	15–18	Middle Ages	22.01	144.00	471.00	4691.20
Humerus	M	18–20	Middle Ages	29.18	214.60	542.20	5044.80
Ulna	M	20–25	Middle Ages	27.39	154.25	421.55	4195.58
Humerus	M	20–25	Middle Ages	26.08	160.47	467.47	5523.00
Radius	M	20–25	Middle Ages	22.18	138.66	543.64	2956.02
Ulna	M	20–25	Middle Ages	19.66	143.01	545.34	2321.58
Radius	M	20–25	Middle Ages	19.07	137.99	546.79	2301.98
Radius	F	20–25	Middle Ages	16.78	151.90	518.59	2493.96
Humerus	F	30–35	Middle Ages	26.93	185.27	491.93	3454.60
Ulna	F	30–35	Middle Ages	26.91	176.19	447.43	3311.75
Radius	M	40–45	Middle Ages	24.09	160.64	492.41	3982.52
Humerus	M	40–45	Middle Ages	28.50	177.33	493.20	6267.80
Radius	M	40–45	Middle Ages	21.61	147.39	473.33	4299.95
Humerus	M	40–50	Middle Ages	25.04	170.33	558.67	4073.40
Ulna	M	40–55	Middle Ages	28.82	180.85	447.79	3320.23
Ulna	M	45–45	Middle Ages	26.04	199.49	409.80	4195.33
Humerus	M	45–50	Middle Ages	25.25	121.20	440.47	3718.20
Ulna	M	45–50	Middle Ages	27.62	171.27	391.52	4352.84
Ulna	M	55+	Middle Ages	31.07	157.65	524.62	4026.97
Radius	F	55+	Middle Ages	22.64	178.68	518.57	2018.25
Ulna	F	55+	Middle Ages	29.09	155.45	443.43	3680.35
Radius	F	55+	Middle Ages	19.12	131.28	536.06	2473.80
Humerus	M	55+	Middle Ages	26.81	166.33	426.33	5589.60
Humerus	F	55+	Middle Ages	28.09	160.00	516.07	6117.20

Table 3. *Cont.*

Bone Name/Group	Sex	Age	Time Period	Mean Bone Volume to Trabecular Volume Ratio (%/0.5 cm^3)	Mean Thickness of Trabecular Bone (μm)	Mean Diameter of Bone Pores (μm)	Mean Thickness of Cortical Bone (μm)
Ulna	F	55+	Middle Ages	30.73	169.69	561.16	4179.27
Ulna	F	55+	Middle Ages	24.23	176.83	480.08	3689.85
Radius	F	55+	Middle Ages	18.54	127.77	467.11	4073.07
Ulna	M	55+	Middle Ages	28.47	178.95	433.84	3628.81
Ulna	M	55+	Middle Ages	31.60	149.97	389.56	4681.52
Ulna	M	55+	Middle Ages	33.85	222.26	347.59	3537.82

A strong positive correlation has been found in Middle Ages bone samples between factors such as OPN and MMP2, OPN and βFGF, and TGFβ and MMP2. A strong positive correlation between factors and some Micro-CT measured parameters was also found—OPN and BV/TV, TIMP2, and Th. of CB, while both—TGFβ and MMP2 revealed a strong negative correlation to the diameter of pores (Table 4). No correlations have been found between factors and the results of Micro-CT scanning in the Late Modern Period group.

Table 4. Spearman's rho shows the strength and direction of association between two analyzed variables (factors, Micro-CT parameters).

Correlation Type		Variable 1	Variable 2	r	*p*-Value
Positive	Strong correlation	OPN	BV/TV	0.772	
		OPN	MMP2	0.730	
		OPN	βFGF	0.716	
		TGFβ	MMP2	0.716	
		TIMP2	Th. of CB	0.687	
Negative	Strong correlation	TGFβ	Diameter of pores	−0.845	
		MMP2	Diameter of pores	−0.678	

Abbreviations: r—correlation coefficient; OPN—osteopontin; TIMP2—tissue inhibitor of metalloproteinases-2; MMP2—matrix metalloproteinase-2; TGFβ—transforming growth factor β; βFGF—β-fibroblast growth factor; BV/TV—Bone volume/Trabecular volume; Th. of CB—thickness of cortical bone.

4. Discussion

This study aimed to analyze the expression of different tissue factors in historic Latvian bones to evaluate and compare their levels between the Late Modern Period and Middle Ages bone samples.

The Micro-CT results of our study have shown that the mean bone volume to trabecular volume ratio was significantly higher in the Late Modern Period group. Meanwhile trabecular thickness, thickness of cortical bone, and mean diameter of bone pores expressed no significant differences between the Late Modern Period and the Middle Ages groups.

Data analysis within one time period revealed that the mean bone volume to trabecular volume ratio and mean thickness of trabecular bone were significantly higher in the 30–55+ years old group than in the 15–25 years old group for the Late Modern Period while the mean diameter of bone pores was significantly lower. The same tendency can be observed for the Late Modern Period where the mean bone volume to trabecular volume ratio and mean thickness of trabecular bone were significantly higher in the 30–55+ years old group than in the 15–25 years old group. For the Middle Ages, only the mean bone

volume to trabecular volume ratio was significantly higher in the 30–55+ years old group than in the 15–25 years old group.

Additionally, there is a statistically significant interaction between age groups (15–25 years old and 30–55+ years old) and time periods (Late Modern Period and Middle Ages) which impacts the mean bone volume to trabecular volume ratio, mean thickness of trabecular bone, and mean diameter of bone pores. In all the cases of interactions, the strength of the effect was at a medium level.

Speaking about sex-related differences, it has been observed that the mean diameter of bone pores was significantly lower in the male group than in the female group during Middle Ages [46].

Moreover, there is a statistically significant interaction between sexes (males and females) and time period (Late Modern Period and Middle Ages) which impacts the mean bone volume to trabecular volume ratio.

Anthropometric differences between populations from the Middle Ages and those from the Late Modern Period can largely be attributed to changes in nutrition, health, and living conditions. As well as it is important to consider that the skeletal remains unearthed at St. George's Church likely belong to individuals of higher socioeconomic status, given the historical fact that only the rich and aristocratic were buried there. These individuals would typically have better access to nutrition and healthcare compared to the lower social classes, which could potentially skew our anthropometric data towards larger body sizes and better overall health compared to the average population.

Moreover, the nature of their lifestyles, particularly the reduced physical labor, could affect their skeletal structures in distinctive ways. Physical labor, such as farming or manual work, can lead to certain markers and changes in the skeleton, including increased robustness or signs of repetitive strain injuries. These would be less likely to appear in individuals from higher classes who did not engage in such work. This could cause further differences when comparing these skeletal remains with those of individuals who performed hard physical labor.

Thus, it's essential to factor in these biases when interpreting the data and drawing conclusions about population health and physical characteristics. The skeletal remains from St. George's Church may not necessarily represent the average medieval person but instead reflect a specific subset of the population.

Physical activity seems to have different effects on cortical and trabecular bones, in response to mechanical forces, the former increases in size, while the latter increases in density [47]. Nilsson et al. [48] observed that in young men the type of physical activity and the associated degree of mechanical loading predominantly affected the trabecular microstructure, whereas the duration of previous physical activity was mainly related to parameters reflecting cortical bone size in weight-bearing bones. Later, Nilsson et al. [49] indicated that the physical activity of elderly women may decrease cortical bone loss in weight-bearing bones. Thus, a greater mean bone volume to trabecular volume ratio in the Late Modern Period group could mean that these individuals have had greater physical loads, as well as a more sufficient diet in later centuries. Studies show that cortical and trabecular porosity, as well as density, are correlated with age-related changes [50] and disease-affected bone loss and fragility [51–53]. Archaeological finds from Riga mainly show the clothes of ordinary citizens, and artifacts found in their graves indicate that people had the same socio-economic status. Since trade in the 14th and 15th centuries was more important than craftwork, we can assume that our study involved human remains belonging to people who do not experience great physical exertion [38]. Women from the middle and lower classes in Riga were involved in various forms of crafts and trade, such as spinning and baking, as well as played important roles in the family economy, helping to tend livestock and selling goods in the local markets [39]. Also, political challenges, such as numerous local wars and sieges of the city, could lead to poor nutrition among the population or even starvation. Therefore, a reason for Middle Ages group bones to have greater pore diameter might be a result of some bone quality changes and/or pathology.

Applying IHC for the evaluation of a variety of tissue factors and cytokines (e.g., TGFβ, OPN, MMP2, TIMP2, OPG, OCN, βFGF, Runx2, IL-1a, IL-10, BMP 2/4, and βDef.2) in bone cells showed the presence of almost all of them, except Runx2. A significant difference was found in the presence of TIMP2, which was more abundant in the Late Modern Period group, while IL-1a positive cell number was significantly higher in the Middle Ages group. Produced by the same bone cells, TIMP-2 is an inhibitor of MMP-2 function [54,55]. The balance between activated MMPs and TIMPs controls the extent of extracellular matrix remodeling, so the imbalance of the MMPs and TIMP2 enzyme expression may lead to pathological processes [56–58]. Miller et al. [59] suggested that the lack of TIMP-3 cause high bone remodeling, which is detrimental to bone development and maintenance. From this, we can infer that the increased presence of TIMP2-positive cells in the specimens from the Late Modern Period could suggest their role in inhibiting the bone resorption activity of MMP2. This may be because individuals from the Late Modern Period group could have had health conditions that led to alterations in TIMP2 levels. And these facts additionally prove the better bone homeostasis/health in the Late Modern Period in comparison to the Middle Ages.

IL-1 is a potent stimulator of bone resorption both in vitro and in vivo. IL-1 provides its resorptive effect on bone by acting directly on osteoclasts and indirectly through stimulation of RANKL production [60]. IL-1 raises the activity of RANKL to stimulate osteoclastogenesis [61] and increases prostaglandin synthesis in bones, which also affects bone reabsorption [60]. IL-1 is produced within bones [62], and its activity is present within the serum of the bone marrow cavity [63]. At first, the only masonry buildings were churches, castles of the Bishop and the Order, and monasteries, while other buildings were made of wood, which was the cause of frequent fires [38], which together with poor medicine could cause many health problems. Therefore, higher values of IL-1a in the Middle Ages group indicate the presence of an inflammation process and, probably, bone resorption. These conclusions are further supported by the fact that even though bones with the least visual damage were selected for this study, after the preparation of microslides with bone sections, signs of small damage were found on the periphery of tissue fragments, mainly in the Middle Ages samples.

Correlation analysis results, both negative and positive, were found only in the Middle Ages group. OPN had a positive correlation toward MMP2, βFGF, and BV/TV. TIMP2 showed an almost significant strong correlation to such Micro-CT measurement as the thickness of cortical bone. In bone tissue, OPN regulates osteoclast differentiation, migration, and activation. It is thought that OPN has a key role in osteoclast adhesion to bone tissue and the formation of a ruffled border zone during the active bone resorption process. During resorption, osteoclasts attach themselves to the unresorbed bone matrix through the αvβ3-integrin receptor. It is thought that the RGD sequence found in OPN is one of the key ligands for the receptor in the bone matrix [64,65]. Research has shown that OPN increases osteoclast proliferation and differentiation but reduces osteoblast proliferation and differentiation [66]. Recent evidence has demonstrated that human osteoclasts secrete OPN into resorption lacunae on human bone and on carbonated hydroxyapatite, which does not have any natural OPN. The possible function of OPN could be chemokine activity for further bone formation [67]. In turn, MMP-2 is mainly expressed in osteoblasts and osteoclasts, which have an important role in bone absorption [68]. MMP-2, together with MMP-1, degrades collagen type I, the major structural component of the bone organic matrix [69]. Research shows that MMPs serve a critical role in osteoclastic bone resorption and facilitate the migration of osteoclasts to bone surfaces via the extracellular matrix [70]. The MMP-2 protein activates bone absorption by enhancing the osteoclast MMP-2 activity and promoting the degradation of the bone matrix [71] or through the degradation of the type I collagen barrier under the osteoblasts and further activation of osteoclast functions [72]. The basic fibroblast growth factor (BFGF) is a growth factor that regulates cell growth, differentiation, and metabolism. BFGF has been found to be expressed and has in vitro activity and gene function in the process of angiogenesis, hematopoietic cells, chondrocytes,

and osteoblasts, both in adults and during embryonic development. BFGF within cartilage and bone is necessary for the morphogenesis, mineralization, and metabolism of these tissues [14].

A positive correlation was also found between TGF-β and MMP2. TGF-β and the related group of proteins BMPs play an important role in the process of bone formation during mammalian development. These proteins demonstrate variable regulatory functions within the body [9]. TGF-β provides autocrine and paracrine stimulation that is important for the maintenance and expansion of mesenchymal stem cells (MSCs), the progenitors of osteoblasts. Bone and cartilage tissue contains the target cells for TGF-β activity and relatively large amounts of TGF-β within the tissue [73]. TGF-β1, β2, and β3 have multiple effects on osteoblastic cells that depend on the timing, dosage, and context of the presence of these growth factors. These factors affect osteoblast differentiation stages differentially [74].

A negative correlation between TGFβ, MMP2, and the diameter of pores indicates that, in case of a rise in TGFβ secretion, it will induce osteoblast activity and form new bone tissue, which as a result can reduce pore diameter between trabecular bones. In the case of MMP2, whose correlation was close to being significant, its increase will induce bone absorption, which will cause TIMP2 synthesis too; to balance this process, in this case, the diameter of pores can again become smaller.

However, we realize the limitations of our manuscript. The article could be strengthened by expanding the sample size within each group through the inclusion of human remains from other excavations in Riga that belong to the same historical time periods. Increasing the number of samples would enhance the article's overall validity and contribute to a more comprehensive understanding of anthropometric measurements during the specified time periods. In the pursuit of comparative research between the bone quality, exploring the bone density and protein concentrations could offer intriguing insights.

Those examinations would not only provide us with a more comprehensive understanding of historical dietary and lifestyle factors but could also establish an innovative methodological approach for future archaeological investigations. Determining such biological factors may indeed be a rewarding direction for this study, adding another layer of depth to our understanding of human health and lifestyle changes across these two distinct periods.

5. Conclusions

Archaeological Latvian human bone remains of the Middle Ages period demonstrated a decrease in mean bone volume to trabecular volume ratio in comparison with the Late Modern Period, suggesting decreased bone quality in skeletons, possibly associated with a poorer standard of living during this time period. Other measurements have not demonstrated statistically significant results. However, there is a tendency for the measurements (mean bone volume to trabecular volume ratio, mean thickness of trabecular bone, mean diameter of bone pores, and mean thickness of cortical bone) to be higher in the male group in comparison to the female group.

The decrease in BMP2/4, TGFbeta, and TIMP-2 indicates the disturbances in skeletal bone development/growth and remodeling in Middle Ages humans in Latvia may be caused by the unstable political situation and problems with provisions.

The increase in IL-1 and decrease in IL-10 indicate the more distinct bone resorption on the diminished local anti-inflammatory prone in the Middle Ages, which should be related to the environment and poor medicine of that time period.

Author Contributions: Conceptualization, M.P.; methodology, K.Š., M.P., M.Z. and E.E.; validation, M.P.; formal analysis, K.Š. and E.E.; investigation, K.Š., M.P. and M.Z.; resources, M.P.; data curation, K.Š. and E.E.; writing—original draft preparation, K.Š.; writing—review and editing, M.P.; visualization, E.E.; supervision, M.P.; project administration, M.P. All authors have read and agreed to the published version of the manuscript.

References

1. Feng, X. Chemical and Biochemical Basis of Cell-Bone Matrix Interaction in Health and Disease. *Curr. Chem. Biol.* **2009**, *3*, 189–196.
2. Bonewald, L.F. The amazing osteocyte. *J. Bone Miner. Res.* **2001**, *26*, 229–238. [CrossRef] [PubMed]
3. Chen, H.; Senda, T.; Kubo, K.Y. The osteocyte plays multiple roles in bone remodeling and mineral homeostasis. *Med. Mol. Morphol.* **2015**, *48*, 61–68. [CrossRef] [PubMed]
4. Bell, L.S.; Kayser, M.; Jones, C. The mineralized osteocyte: A living fossil. *Am. J. Phys. Anthropol.* **2008**, *137*, 449–456. [CrossRef]
5. Florencio-Silva, R.; Sasso, G.R.; Sasso-Cerri, E.; Simões, M.J.; Cerri, P.S. Biology of Bone Tissue: Structure, Function, and Factors That Influence Bone Cells. *BioMed Res. Int.* **2015**, *2015*, 421746. [CrossRef]
6. Kenkre, J.S.; Bassett, J. The bone remodelling cycle. *Ann. Clin. Biochem.* **2018**, *55*, 308–327. [CrossRef] [PubMed]
7. Tresguerres, F.G.F.; Torres, J.; López-Quiles, J.; Hernández, G.; Vega, J.A.; Tresguerres, I.F. The osteocyte: A multifunctional cell within the bone. *Ann. Anat.* **2020**, *227*, 151422. [CrossRef]
8. Komori, T. Regulation of Proliferation, Differentiation and Functions of Osteoblasts by Runx2. *Int. J. Mol. Sci.* **2019**, *20*, 1694. [CrossRef]
9. Chen, G.; Deng, C.; Li, Y.P. TGF-β and BMP signaling in osteoblast differentiation and bone formation. *Int. J. Biol. Sci.* **2012**, *8*, 272–288. [CrossRef]
10. Xiao, W.; Wang, Y.; Pacios, S.; Li, S.; Graves, D.T. Cellular and Molecular Aspects of Bone Remodeling. *Front. Oral Biol.* **2016**, *18*, 9–16.
11. Heino, T.J.; Hentunen, T.A.; Väänänen, H.K. Osteocytes inhibit osteoclastic bone resorption through transforming growth factor-beta: Enhancement by estrogen. *J. Cell. Biochem.* **2002**, *85*, 185–197. [CrossRef]
12. Bosetti, M.; Boccafoschi, F.; Leigheb, M.; Cannas, M.F. Effect of different growth factors on human osteoblasts activities: A possible application in bone regeneration for tissue engineering. *Biomol. Eng.* **2007**, *24*, 613–618. [CrossRef]
13. Montero, A.; Okada, Y.; Tomita, M.; Ito, M.; Tsurukami, H.; Nakamura, T.; Doetschman, T.; Coffin, J.D.; Hurley, M.M. Disruption of the fibroblast growth factor-2 gene results in decreased bone mass and bone formation. *J. Clin. Investig.* **2000**, *105*, 1085–1093. [CrossRef] [PubMed]
14. Coffin, J.D.; Homer-Bouthiette, C.; Hurley, M.M. Fibroblast Growth Factor 2 and Its Receptors in Bone Biology and Disease. *J. Endocr. Soc.* **2008**, *2*, 657–671. [CrossRef]
15. Paiva, K.B.S.; Granjeiro, J.M. Matrix Metalloproteinases in Bone Resorption, Remodeling, and Repair. *Prog. Mol. Biol. Transl. Sci.* **2017**, *148*, 203–303.
16. Kumar, G.; Roger, P.M. From Crosstalk between Immune and Bone Cells to Bone Erosion in Infection. *Int. J. Mol. Sci.* **2019**, *20*, 5154. [CrossRef] [PubMed]
17. Schmidt-Schultz, T.H.; Schultz, M. Bone protects proteins over thousands of years: Extraction, analysis, and interpretation of extracellular matrix proteins in archeological skeletal remains. *Am. J. Phys. Anthropol.* **2004**, *123*, 30–39. [CrossRef] [PubMed]
18. Schmidt-Schultz, T.H.; Schultz, M. Well preserved non-collagenous extracellular matrix proteins in ancient human bone and teeth. *Int. J. Osteoarch.* **2007**, *17*, 91–99. [CrossRef]
19. Schmidt-Schultz, T.H.; Schultz, M. Intact growth factors are conserved in the extracellular matrix of ancient human bone and teeth: A storehouse for the study of human evolution in health and disease. *Biol. Chem.* **2005**, *386*, 767–776. [CrossRef] [PubMed]
20. Smith, C.I.; Craig, O.E.; Prigodich, R.V.; Nielsen-Marsh, C.M.; Jans, M.M.E.; Vermeer, C.; Collins, M.J. Diagenesis and survival of osteocalcin in archaeological bone. *J. Arch. Sci.* **2005**, *32*, 105–113. [CrossRef]
21. Scott, A.B.; Alberto, J.; Taurozzi, A.J.; Hughes, N.; Pedersen, D.D.; Kontopoulos, I.; Mackie, M.; Collins, M.J. Comparing biological and pathological factors affecting osteocalcin concentrations in archaeological skeletal remains. *J. Arch. Sci.* **2020**, *34*, 102573. [CrossRef]
22. Caruso, V.; Cummaudo, M.; Maderna, E.; Cappella, A.; Caudullo, G.; Scarpulla, V.; Cattaneo, C. A comparative analysis of microscopic alterations in modern and ancient undecalcified and decalcified dry bones. *Am. J. Phys. Anthropol.* **2018**, *165*, 363–369. [CrossRef]
23. Miszkiewicz, J.J.; Mahoney, P. Ancient Human Bone Microstructure in Medieval England: Comparisons between Two Socio-Economic Groups. *Anat. Rec.* **2016**, *299*, 42–59. [CrossRef]

24. Beresheim, A.C.; Pfeiffer, S.; Grynpas, M. Ontogenetic changes to bone microstructure in an archaeologically derived sample of human ribs. *J. Anat.* **2020**, *236*, 448–462. [CrossRef]

25. Chappard, D.; Baslé, M.F.; Legrand, E.; Audran, M. Trabecular bone microarchitecture: A review. *Morphologie* **2008**, *92*, 162–170. [CrossRef]

26. Beresheim, A.C.; Pfeiffer, S.K.; Grynpas, M.D.; Alblas, A. Sex-specific patterns in cortical and trabecular bone microstructure in the Kirsten Skeletal Collection, South Africa. *Am. J. Hum. Biol.* **2018**, *30*, e23108. [CrossRef] [PubMed]

27. Kozma, C. Skeletal dysplasia in ancient Egypt. *Am. J. Med. Genet. A* **2008**, *146*, 3104–3112. [CrossRef] [PubMed]

28. Kesterke, M.J.; Judd, M.A. A microscopic evaluation of Paget's disease of bone from a Byzantine monastic crypt in Jordan. *Int. J. Paleopathol.* **2019**, *24*, 293–298. [CrossRef]

29. Shaw, B.; Burrell, C.L.; Green, D.; Navarro-Martinez, A.; Scott, D.; Daroszewska, A.; van't Hof, R.; Smith, L.; Hargrave, F.; Mistry, S.; et al. Molecular insights into an ancient form of Paget's disease of bone. *Proc. Natl. Acad. Sci. USA* **2019**, *116*, 10463–10472. [CrossRef] [PubMed]

30. Bajon, K.; Smiszkiewicz-Skwarska, A.; Stolarczyk, H.; Zygmunt, A.; Rutkowski, M.; Sewerynek, E. Evaluation of bone mineral density on the basis of the results of studies of selected skeleton populations from the microregion of Brześć Kujawski. *Endokrynol. Pol.* **2006**, *57*, 494–500.

31. Stride, P.J.; Patel, N.; Kingston, D. The history of osteoporosis: Why do Egyptian mummies have porotic bones? *J. R. Coll. Phys. Edinb.* **2013**, *43*, 254–261. [CrossRef]

32. Chirchir, H.; Kivell, T.L.; Ruff, C.B.; Hublin, J.J.; Carlson, K.J.; Zipfel, B.; Richmond, B.G. Recent origin of low trabecular bone density in modern humans. *Proc. Natl. Acad. Sci. USA* **2015**, *112*, 366–371. [CrossRef]

33. Chirchir, H.; Ruff, C.B.; Junno, J.A.; Potts, R. Low trabecular bone density in recent sedentary modern humans. *Am. J. Phys. Anthropol.* **2017**, *162*, 550–560. [CrossRef] [PubMed]

34. Gosman, J.H.; Ketcham, R.A. Patterns in ontogeny of human trabecular bone from SunWatch Village in the Prehistoric Ohio Valley: General features of microarchitectural change. *Am. J. Phys. Anthropol.* **2009**, *138*, 318–332. [CrossRef] [PubMed]

35. Pitfield, R.; Deter, C.; Mahoney, P. Bone histomorphometric measures of physical activity in children from medieval England. *Am. J. Phys. Anthropol.* **2019**, *169*, 730–746. [CrossRef] [PubMed]

36. Vinci, R.; Rebaudi, A.; Capparè, P.; Gherlone, E. Microcomputed and Histologic Evaluation of Calvarial Bone Grafts: A Pilot Study in Humans. *Int. J. Periodontics Restor. Dent.* **2011**, *31*, e29–e36.

37. Zeids, T. *Feodālā Rīga*; Zinātne: Riga, Latvia, 1978; pp. 48–53.

38. Celmiņš, A. *Zemē Apslēptā Pilsēta: Izstade par 1991–1997. Gada Arheoloğiskajiem Atrdumiem Rīgā = A City under the Ground: An Exhibition of Archaeological Finds from Riga, 1991–1997*; Dizaina un drukas apgāds: Rīga, Latvia, 1998; ISBN 978-9984-9116-2-5.

39. Šterns, I. *Latvijas Vēsture 1290–1500*; Daugava: Riga, Latvia, 1997; pp. 98–177.

40. Krastiņš, J. *Rīga 1860–1917*; Zinātne: Riga, Latvia, 1978; pp. 22–45.

41. Habbal, O. The Science of Anatomy: A historical timeline. *Sultan Qaboos Univ. Med. J.* **2017**, *17*, e18–e22. [CrossRef]

42. Walker, E.C.; McGregor, N.E.; Chan, A.S.M.; Sims, N.A. Measuring Bone Volume at Multiple Densities by Micro-computed Tomography. *Bio Protoc.* **2021**, *11*, e3873. [CrossRef]

43. Idleburg, C.; Lorenz, M.R.; DeLassus, E.N.; Scheller, E.L.; Veis, D.J. Immunostaining of Skeletal Tissues. *Methods Mol. Biol.* **2021**, *2221*, 261–273.

44. Meyerholz, D.K.; Beck, A.P. Principles and approaches for reproducible scoring of tissue stains in research. *Lab. Investig.* **2018**, *98*, 844–855. [CrossRef]

45. Pilmane, M.; Sidhoma, E.; Akota, I.; Kazoka, D. Characterization of Cytokines and Proliferation Marker Ki67 in Cleft Affected Lip Tissue. *Medicina* **2019**, *55*, 518. [CrossRef] [PubMed]

46. Augat, P.; Schorlemmer, S. The Role of Cortical Bone and Its Microstructure in Bone Strength. *Age Ageing* **2006**, *35*, ii27–ii31. [CrossRef] [PubMed]

47. Ducher, G.; Reduce, S.; Courteix, D.; Benhamou, C.L. Cortical and trabecular bone at the forearm show different adaptation patterns in response to tennis playing. *J. Clin. Densitom.* **2004**, *7*, 399–405. [CrossRef] [PubMed]

48. Nilsson, M.; Ohlsson, C.; Sundh, D.; Mellström, D.; Lorentzon, M. Association of physical activity with trabecular microstructure and cortical bone at distal tibia and radius in young adult men. *J. Clin. Endocrinol. Metab.* **2010**, *95*, 2917–2926. [CrossRef] [PubMed]

49. Nilsson, M.; Sundh, D.; Mellström, D.; Lorentzon, M. Current Physical Activity Is Independently Associated with Cortical Bone Size and Bone Strength in Elderly Swedish Women. *J. Bone Miner. Res.* **2017**, *32*, 473–485. [CrossRef]

50. Vilayphiou, N.; Boutroy, S.; Sornay-Rendu, E.; Van Rietbergen, B.; Chapurlat, R. Age-related changes in bone strength from HR-pQCT derived microarchitectural parameters with an emphasis on the role of cortical porosity. *Bone* **2016**, *83*, 233–240. [CrossRef]

51. Chen, H.; Kubo, K.Y. Bone three-dimensional microstructural features of the common osteoporotic fracture sites. *World J. Orthop.* **2014**, *5*, 486–495. [CrossRef]

52. Samakkarnthai, P.; Sfeir, J.G.; Atkinson, E.J.; Achenbach, S.J.; Wennberg, P.W.; Dyck, P.J.; Tweed, A.J.; Volkman, T.L.; Amin, S.; Farr, J.N.; et al. Determinants of Bone Material Strength and Cortical Porosity in Patients with Type 2 Diabetes Mellitus. *J. Clin. Endocrinol. Metab.* **2020**, *105*, e3718-29. [CrossRef]

53. Porrelli, D.; Abrami, M.; Pelizzo, P.; Formentin, C.; Ratti, C.; Turco, G.; Grassi, M.; Canton, G.; Grassi, G.; Murena, L. Trabecular bone porosity and pore size distribution in osteoporotic patients—A low field nuclear magnetic resonance and microcomputed tomography investigation. *J. Mech. Behav. Biomed. Mater.* **2022**, *125*, 104933. [CrossRef]

54. Cowell, S.; Knauper, V.; Stewart, M.L.; D'Ortho, M.P.; Stanton, H.; Hembry, R.M.; Lopez-Otin, C.; Reynolds, J.J.; Murphy, G. Induction of matrix metalloproteinase activation cascades based on membrane-type 1 matrix metalloproteinase: Associated activation of gelatinase A, gelatinase B and collagenase 3. *Biochem J.* **1998**, *331*, 453–458. [CrossRef]

55. Brew, K.; Dinakarpandian, D.; Nagase, H. Tissue inhibitors of metalloproteinases: Evolution, structure and function. *Biochim. Biophys. Acta* **2000**, *1477*, 267–283. [CrossRef]

56. Hammani, K.; Blakis, A.; Morsette, D.; Bowcock, A.M.; Schmutte, C.; Henriet, P.; DeClerck, Y.A. Structure and characterization of the human tissue inhibitor of metalloproteinases-2 gene. *J. Biol. Chem.* **1996**, *271*, 25498–25505. [CrossRef]

57. Ryan, M.E.; Ramamurthy, S.; Golub, L.M. Matrix metalloproteinases and their inhibition in periodontal treatment. *Curr. Opin. Periodontol.* **1996**, *3*, 85–96. [PubMed]

58. Paiva, K.B.S.; Granjeiro, J.M. Bone tissue remodeling and development: Focus on matrix metalloproteinase functions. *Arch. Biochem. Biophys.* **2014**, *561*, 74–87. [CrossRef]

59. Miller, B.; Spevak, L.; Lukashova, L.; Javaheri, B.; Pitsillides, A.A.; Boskey, A.; Bou-Gharios, G.; Carriero, A. Altered Bone Mechanics, Architecture and Composition in the Skeleton of TIMP-3-Deficient Mice. *Calcif. Tissue Int.* **2017**, *100*, 631–640. [CrossRef]

60. Lorenzo, J.; Horowitz, M.; Choi, Y. Osteoimmunology: Interactions of the bone and immune system. *Endocr. Rev.* **2008**, *29*, 403–440. [CrossRef]

61. Liao, R.; Feng, Z.; Li, W.; Liu, R.; Xu, X.; Yao, S.; Tian, J. Interleukin-1 induces receptor activator of nuclear factor-κB ligand-independent osteoclast differentiation in RAW264.7 cells. *Exp. Ther. Med.* **2021**, *21*, 640. [CrossRef]

62. Lorenzo, J.A.; Sousa, S.L.; Van Den Brink-Webb, S.E.; Korn, J.H. Production of both interleukin-1 α and β by newborn mouse calvaria cultures. *J. Bone Miner. Res.* **1990**, *5*, 77–83. [CrossRef] [PubMed]

63. Kawaguchi, H.; Pilbeam, C.C.; Vargas, S.J.; Morse, E.E.; Lorenzo, J.A.; Raisz, L.G. Ovariectomy enhances and estrogen replacement inhibits the activity of bone marrow factors that stimulate prostaglandin production in cultured mouse calvaria. *J. Clin. Investig.* **1995**, *96*, 539–548. [CrossRef]

64. Ross, F.P.; Chappel, J.; Alvarez, J.I.; Sander, D.; Butler, W.T.; Farach-Carson, M.C.; Mintz, K.A.; Robey, P.G.; Teitelbaum, S.L.; Cheresh, D.A. Interactions between the bone matrix proteins osteopontin and bone sialoprotein and the osteoclast integrin alpha v beta 3 potentiate bone resorption. *J. Biol. Chem.* **1993**, *268*, 9901–9907. [CrossRef] [PubMed]

65. Ek-Rylander, B.; Andersson, G. Osteoclast migration on phosphorylated osteopontin is regulated by endogenous tartrate-resistant acid phosphatase. *Exp. Cell Res.* **2010**, *316*, 443–451. [CrossRef]

66. Dong, M.; Yu, X.; Chen, W.; Guo, Z.; Sui, L.; Xu, Y.; Shang, Y.; Niu, W.; Kong, Y. Osteopontin Promotes Bone Destruction in Periapical Periodontitis by Activating the NF-κB Pathway. *Cell. Physiol. Biochem.* **2018**, *49*, 884–889. [CrossRef]

67. Luukkonen, J.; Hilli, M.; Nakamura, M.; Ritamo, I.; Valmu, L.; Kauppinen, K.; Tuukkanen, J.; Lehenkari, P. Osteoclasts secrete osteopontin into resorption lacunae during bone resorption. *Histochem. Cell Biol.* **2019**, *151*, 475–487. [CrossRef]

68. Zheng, X.; Zhang, Y.; Guo, S.; Zhang, W.; Wang, J.; Lin, Y. Dynamic expression of matrix metalloproteinases 2, 9 and 13 in ovariectomy-induced osteoporosis rats. *Exp. Ther. Med.* **2018**, *16*, 1807–1813. [CrossRef] [PubMed]

69. Liang, H.P.H.; Xu, J.; Xue, M.; Jackson, C.J. Matrix metalloproteinases in bone development and pathology: Current knowledge and potential clinical utility. *Met. Med.* **2016**, *3*, 93–102. [CrossRef]

70. Samanna, V.; Ma, T.; Mak, T.W.; Rogers, M.; Chellaiah, M.A. Actin polymerization modulates CD44 surface expression, MMP-9 activation, and osteoclast function. *J. Cell. Physiol.* **2007**, *213*, 710–720. [CrossRef]

71. Zhang, P.; Zhong, M. Effects of 17beta-estradiol and progesterone on the expression of matrix metalloproteinases and tissue inhibitors of metalloproteinases in rat osteoblasts. *Acad. J. First Med. Coll. PLA* **2001**, *21*, 929–931.

72. Bachmeier, B.E.; Iancu, C.M.; Jochum, M.; Nerlich, A.G. Matrix metalloproteinases in cancer: Comparison of known and novel aspects of their inhibition as a therapeutic approach. *Exp. Rev. Anticancer Ther.* **2005**, *5*, 149–163. [CrossRef] [PubMed]

73. Derynck, R.; Akhurst, R.J. Differentiation plasticity regulated by TGF-beta family proteins in development and disease. *Nat. Cell Biol.* **2007**, *9*, 1000–1004. [CrossRef]

74. Morikawa, M.; Derynck, R.; Miyazono, K. TGF-β and the TGF-β family: Context-dependent roles in cell and tissue physiology. *Cold Spring Harb. Perspect. Biol.* **2016**, *8*, a021873. [CrossRef]